
Learning Frequency Domain Approximation for Binary Neural Networks

Yixing Xu¹, Kai Han¹, Chang Xu², Yehui Tang^{1,3}, Chunjing Xu¹, Yunhe Wang^{*1}

¹Noah’s Ark Lab, Huawei Technologies

²The University of Sydney, ³Peking University

fyixing.xu, kai.han, xuchunjing, yunhe.wang}@huawei.com

c.xu@sydney.edu.au, yhtang@pku.edu.cn

Abstract

Binary neural networks (BNNs) represent original full-precision weights and activations into 1-bit with sign function. Since the gradient of the conventional sign function is almost zero everywhere which cannot be used for back-propagation, several attempts have been proposed to alleviate the optimization difficulty by using approximate gradient. However, those approximations corrupt the main direction of de facto gradient. To this end, we propose to estimate the gradient of sign function in the Fourier frequency domain using the combination of sine functions for training BNNs, namely frequency domain approximation (FDA). The proposed approach does not affect the low-frequency information of the original sign function which occupies most of the overall energy, and high-frequency coefficients will be ignored to avoid the huge computational overhead. In addition, we embed a noise adaptation module into the training phase to compensate the approximation error. The experiments on several benchmark datasets and neural architectures illustrate that the binary network learned using our method achieves the state-of-the-art accuracy.

1 Introduction

The success of deep convolutional neural networks (CNNs) has been well demonstrated in several real-world applications, *e.g.* , image classification [20, 29], object detection [35], semantic segmentation [28], and low-level computer vision [37]. Massive parameters and huge computational complexity are usually required for achieving the desired high performance, which limits the application of these models to portable devices such as mobile phones and smart cameras.

In order to reduce the computational costs of deep neural networks, a number of works have been proposed to compress and accelerate the original cumbersome model into a portable one. For example, filter pruning methods [27, 43] aim to sort the filters based on their importance scores in which unimportant filters will be treated as redundancy and removed to derive lightweight architectures. Knowledge distillation methods [16, 30] are explored to transfer the knowledge inside a teacher model to a student model. Tensor decomposition method [33] decomposes the original large weight tensor into several small ones to simplify the overall inference process. Model quantization methods [11, 18] quantize the widely used 32-bit floating point weights and activations into low-bit ones to save the memory consumption and computational cost.

Among the aforementioned algorithms, binary neural network (BNN) is an extreme case of model quantization method in which the weights and activations in the original neural network will be quantized to 1-bit (-1 and +1) values. Obviously, the memory usage for weights and activations

*Corresponding author.

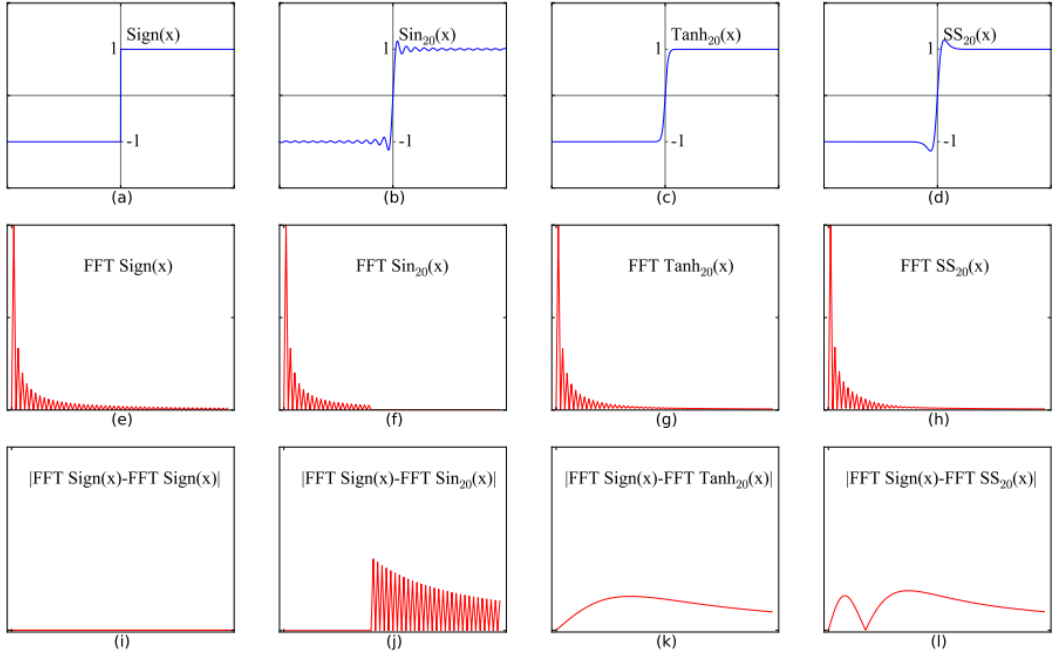


Figure 1: From top to bottom: original functions in spatial domain, corresponding functions in frequency domain and the difference between the current function and sign function in frequency domain. From left to right: sign function, combination of sine functions, tanh function in [8] and SignSwish function in [5] (short as SS).

in BNNs are $32\times$ lower than that in the full-precision network with the same model architecture. BNN was firstly proposed by Hubara *et.al.* [18] by utilizing straight-through estimator (STE) [1] for handling gradient problem of sign function. Then, XNOR-Net [34] introduced a channel-wise scaling factor for weights to reduce the quantization error. Dorefa-Net [42] used a single scaling factor for all the channels and achieved competitive performance. In addition, there are a number of methods for optimizing the original structure to improve the performance of learned BNN. ABCNet [23] used multiple parallel binary convolutional layers. Bi-Real Net [26] inserted skip-connections to enhance the feature representation ability of deep BNNs.

The optimization difficulty caused by the sign function in BNNs is a very important issue. In practice, the original full-precision weights and activations will be quantized into binary ones with sign function during the feed-forward procedure, but the gradient of sign function cannot be directly used for back-propagation. Therefore, most of the approaches mentioned above adopt the straight-through estimator (STE) [1] for gradient back-propagation to train BNNs. The inconsistency between the forward and backward pass caused by the STE method prevents BNN from achieving better performance. Additionally, several attempts were proposed to estimate the gradient of sign function for replacing STE. For example, DSQ [8] introduced a tanh-alike differentiable asymptotic function to estimate the forward and backward procedures of the conventional sign function. BNN+ [5] used a SignSwish activation function to modify the back-propagation of the original sign function and further introduced a regularization that encourages the weights around binary values. RBNN [22] proposed a training-aware approximation function to replace the sign function when computing the gradient. Although these methods have made tremendous effort for refining the optimization of binary weights and activations, the approximation function they used may corrupt the **main direction** of de facto gradient for optimizing BNNs.

To better maintain the main direction of de facto gradient in BNNs, we propose a frequency domain approximation approach by utilizing the Fourier Series (FS) to estimate the original sign function in the frequency domain. The FS estimation is a lossless representation of the sign function when using infinite terms. In practice, the high-frequency coefficients with relatively lower energy will be ignored to avoid the huge computational overhead, and the sign function will be represented as the combination of a fixed number of sine functions with different periods. Compared with the existing

approximation methods, the proposed frequency domain approximation approach does not affect the low-frequency domain information of the original sign function, *i.e.*, the part that occupies most energy of sign function as shown in Fig. 1. Thus, the main direction of the corresponding gradient *w.r.t.* the original sign function can be more accurately maintained. In addition, to further compensate the subtle approximation error, we explore a noise adaptation module in the training phase to refine the gradient. To verify the effectiveness of the proposed method, we conduct extensive experiments on several benchmark datasets and neural architectures. The results show that our method can surpass other state-of-the-art methods for training binary neural networks with higher performance.

2 Approach

In this section, we first provide the preliminaries of BNNs and STE briefly. Then, we propose to estimate sign function with the combination of sine functions and analyze the inaccurate estimation problem. Finally, we introduce a noise adaptation module to solve the problem and derive our FDA-BNN framework.

2.1 Preliminaries

The conventional BNNs quantize the weight matrix $W \in \mathbb{R}^{c_i \times c_o \times k \times k}$ and activation matrix $A \in \mathbb{R}^{b \times c_i \times h \times w}$ to 1-bit, and obtain the binary matrices $W_b \in \mathbb{R}^{c_i \times c_o \times k \times k}$ and $A_b \in \mathbb{R}^{b \times c_i \times h \times w}$ for the intermediate convolution layers using sign function as follows:

$$w_b = \begin{cases} 1, & w_f > 0, \\ -1, & w_f \leq 0, \end{cases} \quad a_b = \begin{cases} 1, & a_f > 0, \\ -1, & a_f \leq 0, \end{cases} \quad (1)$$

where w_f and a_f are the elements in the original 32-bit floating point weight matrix W and activation matrix A , respectively, and w_b and a_b are the elements in the binarized weight matrix W_b and activation matrix A_b , respectively. Given the 1-bit weights and activations, the original convolution operation can be implemented with bitwise XNOR operation and the bit-count operation [26]. During training, both the full-precision weight matrix W and the 1-bit weight matrix W_b are used, while only W_b is kept for inference.

Note that it is hard to apply back-propagation scheme on the sign function. The gradient of sign function is an impulse function that is almost zero everywhere and is unable to be utilized in training. Thus, the STE method [1] is introduced to compute its gradient as:

$$\frac{\partial \mathcal{L}}{\partial w} = Clip\left(\frac{\partial \mathcal{L}}{\partial w_b}, -1, 1\right), \quad (2)$$

in which \mathcal{L} is the corresponding loss function for the current task (*i.e.*, cross-entropy loss for image classification) and

$$Clip(x, -1, 1) = \begin{cases} -1, & \text{if } x < -1, \\ x, & \text{if } -1 \leq x < 1, \\ 1, & \text{otherwise.} \end{cases} \quad (3)$$

Since STE is an inaccurate approximation of the gradient of sign function, many works have focused on replacing STE during back-propagation. BNN+ [5] introduced a SignSwish function, while DSQ [8] proposed a tanh-alike function and minimized the gap between the sign function with a learnable parameter. Such methods focus on approximating sign function in spatial domain, and corrupt the main direction of the gradient. Thus, we propose a new way to estimate sign function to maintain the information in frequency domain.

2.2 Decomposing Sign with Fourier Series

In the following sections, we use $f(\cdot)$ and $f'(\cdot)$ to denote an original function and its corresponding gradient function.

It has been proved in the area of signal processing that any periodical signal with period T can be decomposed into the combination of Fourier Series (FS):

$$f(t) = \frac{a_0}{2} + \sum_{i=1}^{\infty} [a_i \cos(i\omega t) + b_i \sin(i\omega t)], \quad (4)$$

in which $\omega = 2\pi/T$ is the radian frequency, $a_0/2$ is the direct component and $\{b_i\}_{i=1}^{\infty}$ ($\{a_i\}_{i=1}^{\infty}$) are the coefficients of the sine (cosine) components. Specifically, when the periodical signal is the square wave, we have

$$a_i = 0 \text{ for all } i; \quad b_i = \begin{cases} \frac{4}{i\pi}, & \text{if } i \text{ is odd,} \\ 0, & \text{otherwise.} \end{cases} \quad (5)$$

and derive the FS for the square wave $s(t)$:

$$s(t) = \frac{4}{\pi} \sum_{i=0}^{\infty} \frac{\sin((2i+1)\omega t)}{2i+1}. \quad (6)$$

Note that when restricting the signal into a single period, the sign function is exactly the same as the square wave:

$$\text{sign}(t) = s(t), \quad |t| < T. \quad (7)$$

Thus, the sign function can also be decomposed into the combination of sine functions, and its derivative is computed as:

$$s'(t) = \frac{4\omega}{\pi} \sum_{i=0}^{\infty} \cos((2i+1)\omega t). \quad (8)$$

In this way, we propose to replace the derivative used in STE (Eq. 2) with Eq. 8 during back-propagation for better approximating the sign function.

2.3 Inaccurate Estimation Problem in FDA-BNN

The FS decomposition is a lossless representation of the sign function when using infinite terms by transforming the signal from spatial domain into frequency domain, as shown in Theorem 1. First, we can rewrite Eq. 6 as

$$\hat{s}_n(t) = \frac{4}{\pi} \sum_{i=0}^n \frac{\sin((2i+1)\omega t)}{2i+1}, \quad (9)$$

where n is the number of FS terms. The corresponding derivative is

$$\hat{s}'_n(t) = \frac{4\omega}{\pi} \sum_{i=0}^n \cos((2i+1)\omega t). \quad (10)$$

In the following, we show that as n increases, the mean squared error between the estimator $\hat{s}_n(t)$ and the ground-truth $s(t)$ decreases, and converges to 0 when $n \rightarrow \infty$.

Theorem 1. (Mean Square Convergence [36]) Given $s(\cdot)$ as the square wave function which is integrable in a period, and $\hat{s}_n(\cdot)$ is the n^{th} partial sum of the Fourier Series of $s(\cdot)$, then $\hat{s}_n(\cdot)$ converges to $s(\cdot)$ in the mean square sense, i.e.,

$$\frac{1}{T} \int_T ||s(t) - \hat{s}_n(t)||_2^2 dt \rightarrow 0 \quad \text{as } n \rightarrow \infty. \quad (11)$$

The above theorem shows that the estimator $\hat{s}_n(t)$ converges to the ground-truth $s(t)$ when using an infinite number of FS terms, and an error

$$r(t) = s(t) - \hat{s}_n(t) \quad (12)$$

occurs in reality when n is finite. The error comes from the infinite high-order FS terms and has little energy. In practice, we use a fixed number of FS terms for two reasons: 1) We can avoid the huge computational overhead by ignoring the high-frequency coefficients. 2) We can still accurately maintain the main direction of the corresponding gradient w.r.t. the original sign function. Compared to other estimation methods that directly estimate sign function in the spatial domain, our method benefits to the approximation process since the proposed approximation approach does not influence the low-frequency domain information of the original sign function, which occupies most of the energy.

Note that when doing back-propagation in BNN, the gradient of sign function $s'(t)$ is not the optimal choice and is never used as the optimal gradient. However, the optimal gradient $s'^*(t)$ which will

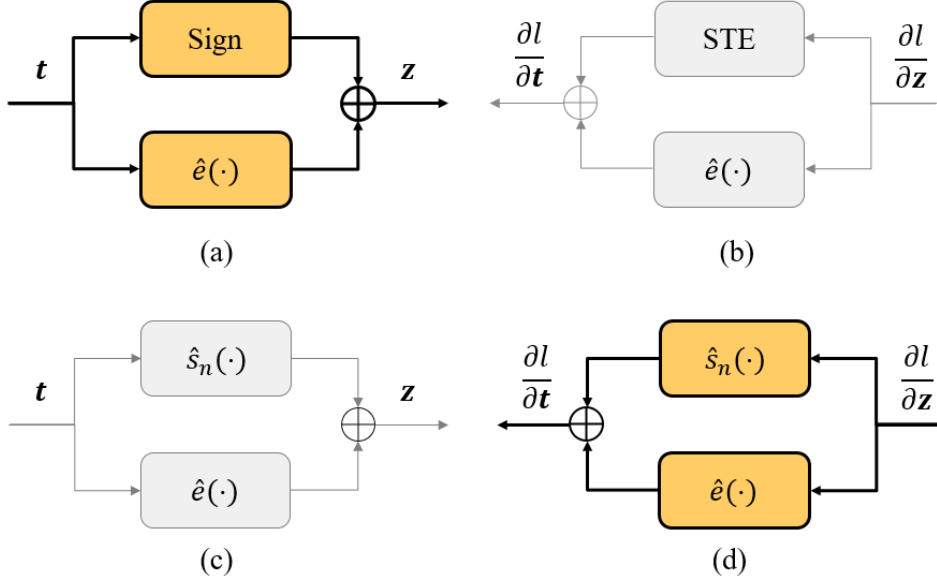


Figure 2: **(a)** The forward pass of the combination of sign function and noise adaptation module. **(b)** Corresponding backward pass of (a). **(c)** The forward pass of the combination of the sine module and the noise adaptation module. **(d)** Corresponding backward pass of (c). The actual forward and backward pass are **bolded** in the figure.

reduce the loss function to the global optimal should not be far away from $s'(t)$. Thus, we can treat $s'(t)$ as contaminating with noise, *i.e.* ,

$$s'(t) = s'^*(t) + n'(t), \quad (13)$$

in which $n'(t)$ is the gradient of unknown noise function $n(t)$. Combining Eq. 12 and Eq. 13, we have:

$$s'^*(t) = \hat{s}'_n(t) + \hat{e}'(t), \quad (14)$$

in which $\hat{e}'(t) = r'(t) - n'(t)$. Thus, the optimal gradient of sign function is divided into two parts. The first part is the gradients of finite number of low-order FS terms which is the main part of the estimation. The second part includes the error from infinite high-order FS terms and noise function, which is inexpressible since $r'(t)$ goes to infinity at $t = 0$ and $n'(t)$ is unknown.

2.4 Solving the Inaccurate Estimation Problem

In the previous works, there are several ways to deal with noise. The first is label correction which correct the wrong labels into the right one [21]. The second is to change the training framework to derive a robust network for noisy labels [13, 12, 40, 7]. The third is to improve the training loss function to a noise robust loss [41].

Different from them, we propose to use a learnable neural network to solve the problem. Specifically, given the input vector $\mathbf{t} \in \mathbb{R}^{1 \times d}$, the process of sign function can be replaced by the combination of a sine module $\hat{s}_n(\cdot)$ and a noise adaptation module $\hat{e}(\cdot)$ which estimates the error $r(\cdot) - n(\cdot)$ using two fully-connected layers with ReLU activation function and a shortcut:

$$\hat{e}(\mathbf{t}) = \sigma(\mathbf{t}W_1)W_2 + \eta(\mathbf{t}), \quad (15)$$

in which $\sigma(t) = \max(t, 0)$, $W_1 \in \mathbb{R}^{d \times \frac{d}{k}}$ and $W_2 \in \mathbb{R}^{\frac{d}{k} \times d}$ are the parameters of the two FC layers in which k is used to reduce the number of parameters and is set to 64 in the following experiments. $\eta(\cdot)$ is the shortcut connection. During the experiment we use different form of $\eta(\cdot)$, details can be found in Sec.3.2.

Note that there are two benefits from adding the shortcut connection. The first is that it helps the flow of gradient and alleviates the gradient vanishing problem [25, 31, 17]. The second is that given

Algorithm 1 Feed-Forward and Back-Propagation Process of a convolutional layer in FDA-BNN.

Require: A convolutional layer with weights W and input features (activations) A , the noise adaptation module with parameters W_{a1} (W_{w1}) and W_{a2} (W_{w2}) for activations (weights), the loss function ℓ_{ce} , the learning rate γ , and training iterations T .

- 1: **for** $\tau = 1$ to T **do**
- 2: **Feed-Forward:**
- 3: Quantize the weights and activations: $W_b = \text{Sign}(W)$, $A_b = \text{Sign}(A)$;
- 4: Apply the convolutional operation on the binarized weights and activations: $W_b \otimes A_b$;
- 5: **Back-Propagation:**
- 6: Compute the gradient of W_b and A_b using standard back-propagation, and get $\frac{\partial \ell_{ce}}{\partial W_b}$ and $\frac{\partial \ell_{ce}}{\partial A_b}$;
- 7: Compute the gradient of A , and derive $\frac{\partial \ell_{ce}}{\partial A}$ using Eq. 17;
- 8: Compute the gradients on parameters of noise adaptation module for activations: $\frac{\partial \ell_{ce}}{\partial W_{a1}}$ and $\frac{\partial \ell_{ce}}{\partial W_{a2}}$ using Eq. 18 and Eq. 19.
- 9: Compute the gradients of W and derive $\frac{\partial \ell_{ce}}{\partial W}$, and also $\frac{\partial \ell_{ce}}{\partial W_{w1}}$ and $\frac{\partial \ell_{ce}}{\partial W_{w2}}$, with the same manner in step 7~8.
- 10: **Parameter Update:**
- 11: $W \leftarrow \text{UpdateParameters}(W, \frac{\partial \ell_{ce}}{\partial W}, \gamma)$;
- 12: $W_{a1} \leftarrow \text{UpdateParameters}(W_{a1}, \frac{\partial \ell_{ce}}{\partial W_{a1}}, \gamma)$
- 13: $W_{a2} \leftarrow \text{UpdateParameters}(W_{a2}, \frac{\partial \ell_{ce}}{\partial W_{a2}}, \gamma)$;
- 14: $W_{w1} \leftarrow \text{UpdateParameters}(W_{w1}, \frac{\partial \ell_{ce}}{\partial W_{w1}}, \gamma)$
- 15: $W_{w2} \leftarrow \text{UpdateParameters}(W_{w2}, \frac{\partial \ell_{ce}}{\partial W_{w2}}, \gamma)$.
- 16: **end for**

$\eta(t) = a \cdot t$ as an example, we have $\eta'(t) = a$ which equals to adding a bias to the gradient. This benefit the training process since given limited training resources and time, only finite number of FS terms n can be used to compute $\hat{s}_n(t)$ in Eq. 9, and raise the problem that the tail of the estimated gradient $\hat{s}'_n(t)$ oscillates around 0 at a very high frequency. This phenomenon does harm to the optimization process, since a very little disturbance on the input will results in two different gradients with opposite direction, and adding a bias term on the gradient helps to alleviate this problem.

Based on the analysis above, given Eq. 9 and Eq. 15, we are able to approximate sign function with the combination of sine module and noise adaptation module:

$$\mathbf{z} = \hat{s}_n(\mathbf{t}) + \alpha \hat{e}(\mathbf{t}), \quad (16)$$

in which α is the hyper-parameter to control the influence of noise adaptation module.

In order to keep the weights and activations as 1-bit in inference, the sine module is used only in the backward pass and replaced as sign function in the forward pass, as shown in Fig. 2. Besides, α is gradually decreased during training and reaches 0 at the end of training to avoid the inconsistency between training phase and inference phase. The weights of both BNN and noise adaptation module are updated in an end-to-end manner by minimizing the cross-entropy loss ℓ_{ce} .

Specifically, given Eq. 16 and the loss function ℓ_{ce} , the gradients in Fig. 2 (d) can be computed as:

$$\begin{aligned} \frac{\partial \ell_{ce}}{\partial \mathbf{t}} &= \frac{\partial \ell_{ce}}{\partial \mathbf{z}} W_2^\top \odot ((\mathbf{t} W_1) \geq 0) W_1^\top + \frac{\partial \ell_{ce}}{\partial \mathbf{z}} \eta'(\mathbf{t}) \\ &+ \frac{\partial \ell_{ce}}{\partial \mathbf{z}} \odot \frac{4\omega}{\pi} \sum_{i=0}^n \cos((2i+1)\omega \mathbf{t}), \end{aligned} \quad (17)$$

in which $\frac{\partial \ell_{ce}}{\partial \mathbf{z}}$ is the gradient back-propagated from the upper layers, \odot represents element-wise multiplication, and $\frac{\partial \ell_{ce}}{\partial \mathbf{t}}$ is the partial gradient on \mathbf{t} that back-propagates to the former layer.

Table 1: Experimental results on CIFAR-10 using different 1-bit quantized models. Bit-width (W/A) denotes the bit length of weights and activations, and BackProp denotes the way of computing gradients and updating parameters.

Network	Method	Bit-width (W/A)	BackProp	Acc (%)
ResNet-20	FP32	32/32	-	92.10
	Dorefa-Net [42]	1/1	STE	84.44
	XNOR-Net [34]	1/1	STE	85.23
	LNS [14]	1/1	STE	85.78
	TBN [38]	1/2	STE	84.34
	DSQ [8]	1/1	Tanh-alike	84.11
	IR-Net [32]	1/1	Tanh-alike	85.40
VGG-small	FDA-BNN	1/1	Fourier Series	86.20
	FP32	32/32	-	94.10
	Dorefa-Net [42]	1/1	STE	90.20
	BinaryNet [18]	1/1	STE	89.90
	XNOR-Net [34]	1/1	STE	89.80
	BNN+ [5]	1/1	SignSwish	91.31
	DSQ [8]	1/1	Tanh-alike	91.72
IR-Net [32]	1/1	Tanh-alike	90.40	
	FDA-BNN	1/1	Fourier Series	92.54

$$\frac{\partial \ell_{ce}}{\partial W_1} = \mathbf{t}^\top \frac{\partial \ell_{ce}}{\partial \mathbf{z}} W_2^\top \odot ((\mathbf{t}W_1) \geq 0); \quad (18)$$

$$\frac{\partial \ell_{ce}}{\partial W_2} = \sigma(\mathbf{t}W_1)^\top \frac{\partial \ell_{ce}}{\partial \mathbf{z}}, \quad (19)$$

in which $\frac{\partial \ell_{ce}}{\partial W_1}$ and $\frac{\partial \ell_{ce}}{\partial W_2}$ are gradients used to update the parameters in the noise adaptation module.

The formulations from Eq. 9 to Eq. 19 are applied for both weights and activations for replacing the back-propagation of sign function. The feed-forward and back-propagation process of a convolutional layer in FDA-BNN is summarized in Alg. 1.

3 Experiments

In this section, we evaluate the proposed method on several benchmark datasets such as CIFAR-10 [19] and ImageNet [6] to show the superiority of FDA-BNN. All of the proposed FDA-BNN models follow the rule in previous methods that all the convolutional layers except the first and last layers are binarized [42, 3, 5].

3.1 Experiments on CIFAR-10

The CIFAR-10 [19] dataset contains 50,000 training images and 10,000 test images from 10 different categories. Each image is of size 32×32 with RGB color channels. Data augmentation methods such as random crop and random flip are used during training. During the experiments, we train the models for 400 epochs with a batch size of 128 and set the initial learning rate as 0.1. The SGD optimizer is used with momentum set of 0.9 and weight decay of 1e-4.

The widely-used ResNet-20 and VGG-Small architectures in BNN literature [26, 8] are used to demonstrate the effectiveness of the proposed method. Dorefa-Net [42] is used as our baseline quantization method, and the sine module and noise adaptation module are used during training. Other competitors include: 1) methods using STE for back-propagation, *e.g.*, BNN [18], Dorefa-Net [42], XNOR-Net [3], TBN [38]; 2) methods using approximated gradient rather than STE during

Table 2: Ablation study on sine module and noise adaptation module.

Sine Module	Noise Adaptation Module	Acc (%)
✗	✗	84.44
✓	✗	85.83
✓	✓	86.20

back-propagation, *e.g.* , DSQ [8], BNN+ [5], IR-Net [32]; 3) fine-tuning methods, *e.g.* , LNS [14]. The experimental results are shown in Tab. 1.

The results show that the proposed FDA-BNN method outperforms all the competitors and achieves state-of-the-art accuracy. For ResNet-20 architecture, the proposed FDA-BNN achieves an accuracy of 86.20% which improves the baseline model by 1.76%, and is 0.42% higher than the previous SOTA method LNS [14] which is a fine-tuning based method and costs 120 more epochs than our method. When applying the proposed method to VGG-small model, the proposed method achieves an accuracy of 92.54% which is also the highest and improves the baseline model by 2.34%. FDA-BNN method outperforms other gradient estimation methods which approximate sign function in spatial domain such as DSQ [8], BNN+ [5] and IR-Net [32].

3.2 Ablation Study

In this section, we conduct several ablation studies to further verify the effectiveness of each component in the proposed method, the impact of shortcut in noise adaptation module and the effect of hyper-parameters.

Firstly, we conduct experiments to understand the effect of sine module and noise adaptation module. The models are verified on CIFAR-10 using ResNet-20 architecture. As shown in Tab. 2, the first line represent the standard Dorefa-Net baseline. We can see that only use sine module can benefit the training process and improve the accuracy from 84.44% to 85.83%. When combining the sine module and noise adaptation module together, we reach the best performance, *i.e.* , 86.20% accuracy, which shows the priority of using both modules in FDA-BNN method during training.

In order to further verify the usefulness of the noise adaptation module, we plug the module into other gradient approximation methods such as DSQ [8] and BNN+ [5]. The experiments are conducted on CIFAR-10 dataset with ResNet-20 model, and the results in Tab. 3 show that fitting the error between the estimated gradient and optimal gradient benefits to different gradient approximation methods.

Table 3: Plugging noise adaptation module into different methods.

	w/o noise module	w/ noise module
DSQ	84.11	84.46
BNN+	84.59	84.87
FDA-BNN	85.83	86.20

Then we evaluate the influence of using different $\eta(\cdot)$ on the branch of shortcut in noise adaptation module. As shown in Tab. 4, using shortcut results in a better performance than not using it, and the shortcut function $\eta(x) = a \sin(x)$ performs the best during the experiment. Note that this is consistent to the analysis in Sec.2.3. Given $\eta(x) = a \sin(x)$, the gradient flow can still be strengthened. Besides, the gradient $\eta'(x) = a \cos(x)$ equals to adding a positive bias in the given range, and thus can still alleviate the problem that the tail of the estimated gradient $\hat{s}'_n(x)$ oscillates around 0 with a very high frequency. a is set to 0.1 during the experiment.

Table 4: Ablation study on $\eta(\cdot)$.

Functions of shortcut branch	Acc (%)
$\eta(x) = 0$ (w/o shortcut)	85.27
$\eta(x) = ax$	85.93
$\eta(x) = a \sin(x)$	86.20

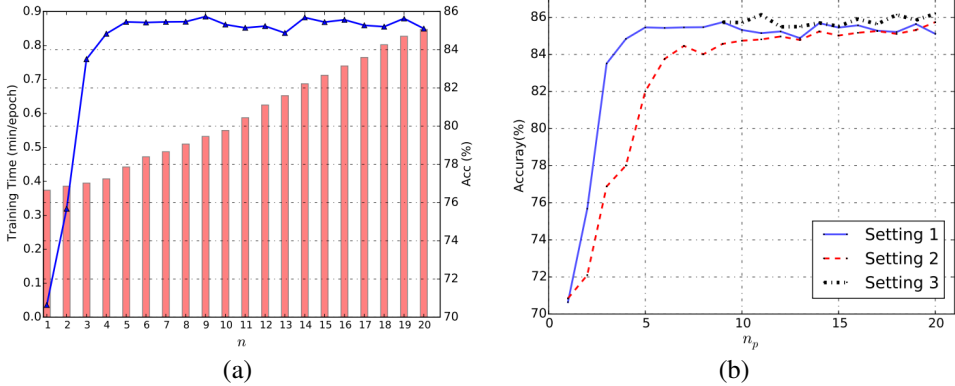


Figure 3: (a) Training time spent and the final accuracy achieved when using different number of FS terms. The blue line denotes the accuracy and the red bar denotes the training time. (b) Accuracies under different settings of hyper-parameter n during training.

Using different number of FS terms during training will influence the final performance of BNN. Intuitively, a larger n will reduce the difference between $\hat{s}_n(\cdot)$ and $sign(\cdot)$, but at the same time lead to more time on training since a combination of n gradients will be computed (Eq. 10). We show the training time spent and the final accuracy achieved by using different n in Fig. 3 (a). We can see that as the number of FS terms n increases, the training time continues to increase while the accuracy saturates at about $n = 10$, which means a moderate n is enough for training an accurate BNN.

As shown in Fig. 3 (a), a small number of FS terms do harm to the performance of BNN while a large n leads to a waste of resources and time. Hence, we explore three different settings of using hyper-parameter n during training.

- Setting 1: the number of FS terms n is fixed to a pre-defined number n_p during training.
- Setting 2: the number of FS terms n is gradually increased from 1 to a pre-defined number n_p .
- Setting 3: the number of FS terms n is gradually increased from 10 (best result in setting 1) to a pre-defined number n_p .

Results of different settings are shown in Fig. 3 (b). Setting 1 performs well at a wider range than setting 2 and they reach a comparable performance when n_p is large enough. Setting 3 performs the best, since it start from a moderate n and avoid the large gap between $\hat{s}_n(\cdot)$ and $sign(\cdot)$ at the beginning of training, and is able to approach the sign function as the training proceed. Thus, in the following experiments we start n from a moderate number n_s (e.g., $n_s = 10$) and gradually increase it to $n_p = 2n_s$.

3.3 Experiments on ImageNet

In this section, we conduct experiments on the large-scale ImageNet ILSVRC 2012 [6] dataset. ImageNet dataset contains over 1.2M training images with 224×224 resolutions from 1,000 different categories, and 50k validation images. The commonly used data augmentation method is applied during training. The training images are resized, random cropped, random flipped and normalized before training, while the test images are resized, center cropped and normalized.

In the following, we conduct experiments on widely-used ResNet-18 and AlexNet. We use the Adam optimizer with momentum of 0.9 and set the weight decay to 0. The learning rate starts from 1e-3. The experimental results are shown in Tab. 5. Following the acknowledged setting [18, 42], the first and last layers of the network are not binarized for classification, and all methods shown in the table except for ABCNet [23] and Binary-Net [17] do not quantize the down-sample layers in the ResNet shortcut branch.

We can see that on ResNet-18, the proposed FDA-BNN achieves a top-1 accuracy of 60.2% and top-5 accuracy of 82.3%, which improves the baseline method (Bireal-Net + PReLU activation function) by 1.2% and 1.0%, and surpass all other competitors including TBN [38] and HWGQ [4] which use

Table 5: Experimental results on ImageNet using different 1-bit quantization methods. ‘W/A’ denotes the bit-width of weights and activations, and BackProp denotes the way of computing gradients and updating parameters.

Network	Method	W/A	BackProp	Top-1 (%)	Top-5 (%)
ResNet-18	FP32	32/32	-	69.6	89.2
	TBN [38]	1/2	STE	55.6	79.0
	Dorefa-Net [42]	1/1	STE	52.5	67.7
	Binary-Net [18]	1/1	STE	42.2	67.1
	XNOR-Net [34]	1/1	STE	51.2	73.2
	ABCNet [23]	1/1	STE	42.7	67.6
	Bireal-Net [26]	1/1	STE	56.4	79.5
	Bireal-Net [26]+PReLU	1/1	STE	59.0	81.3
	BOP [15]	1/1	STE	54.2	77.2
	LNS [14]	1/1	STE	59.4	81.7
	HWGQ [4]	1/2	Piece-wise function	59.6	82.2
	PCNN ($J = 1$) [9]	1/1	DBPP	57.3	80.0
	Quantization Networks [39]	1/1	Sigmoid	53.6	75.3
	ResNetE [2]	1/1	ApproxSign	58.1	80.6
AlexNet	BONN [10]	1/1	Bayesian learning	59.3	81.6
	IR-Net [32]	1/1	Tanh-alike	58.1	80.0
	RBCN [24]	1/1	Project-based	59.5	81.6
	FDA-BNN	1/1	Fourier Series	60.2	82.3
	FP32	32/32	-	56.6	80.2
AlexNet	Dorefa-Net [42]	1/1	STE	43.6	-
	BinaryNet [18]	1/1	STE	41.2	65.6
	XNOR-Net [34]	1/1	STE	44.2	69.2
	LNS [14]	1/1	STE	44.4	-
	FDA-BNN	1/1	Fourier Series	46.2	69.7

2-bit activations for quantization. For AlexNet, we use the quantization method in Dorefa-Net [42] as the baseline method, and achieve a top-1 accuracy of 46.2% and top-5 accuracy of 69.7%, which also outperforms other state-of-the-art methods such as LNS [14] by 1.8% on top-1 accuracy, which shows the superiority of the proposed FDA-BNN method.

4 Conclusion

In this paper, we propose a new frequency domain algorithm (*i.e.*, FDA-BNN) to approximate the gradient of the original sign function in the Fourier frequency domain using the combination of a series of sine functions, which does not affect the low-frequency part of the original sign function that occupies most of the energy. Besides, since only finite FS terms are used in reality, a noise adaptation module is applied to fit the error from the infinite high-order FS terms and the noise occurred between the gradient of sign function and the optimal gradient. In order to gradually approach the sign function, we increase the number of FS terms n during the training. The experimental results on CIFAR-10 and ImageNet datasets using various network architectures demonstrate the effectiveness of the proposed method. Binary networks trained using our method achieve the state-of-the-art performance.

References

- [1] Yoshua Bengio, Nicholas Léonard, and Aaron Courville. Estimating or propagating gradients through stochastic neurons for conditional computation. *arXiv preprint arXiv:1308.3432*, 2013.
- [2] Joseph Bethge, Haojin Yang, Marvin Bornstein, and Christoph Meinel. Back to simplicity: How to train accurate bnnns from scratch? *arXiv preprint arXiv:1906.08637*, 2019.

- [3] Adrian Bulat and Georgios Tzimiropoulos. Xnor-net++: Improved binary neural networks. *arXiv preprint arXiv:1909.13863*, 2019.
- [4] Zhaowei Cai, Xiaodong He, Jian Sun, and Nuno Vasconcelos. Deep learning with low precision by half-wave gaussian quantization. In *Proceedings of the IEEE conference on computer vision and pattern recognition*, pages 5918–5926, 2017.
- [5] Sajad Darabi, Mouloud Belbahri, Matthieu Courbariaux, and Vahid Partovi Nia. Bnn+: Improved binary network training. *arXiv preprint arXiv:1812.11800*, 2018.
- [6] Jia Deng, Wei Dong, Richard Socher, Li-Jia Li, Kai Li, and Li Fei-Fei. Imagenet: A large-scale hierarchical image database. In *2009 IEEE conference on computer vision and pattern recognition*, pages 248–255. Ieee, 2009.
- [7] Jacob Goldberger and Ehud Ben-Reuven. Training deep neural-networks using a noise adaptation layer. 2016.
- [8] Ruihao Gong, Xianglong Liu, Shenghu Jiang, Tianxiang Li, Peng Hu, Jiazen Lin, Fengwei Yu, and Junjie Yan. Differentiable soft quantization: Bridging full-precision and low-bit neural networks. In *Proceedings of the IEEE International Conference on Computer Vision*, pages 4852–4861, 2019.
- [9] Jiaxin Gu, Ce Li, Baochang Zhang, Jungong Han, Xianbin Cao, Jianzhuang Liu, and David Doermann. Projection convolutional neural networks for 1-bit cnns via discrete back propagation. In *Proceedings of the AAAI Conference on Artificial Intelligence*, volume 33, pages 8344–8351, 2019.
- [10] Jiaxin Gu, Junhe Zhao, Xiaolong Jiang, Baochang Zhang, Jianzhuang Liu, Guodong Guo, and Rongrong Ji. Bayesian optimized 1-bit cnns. In *Proceedings of the IEEE International Conference on Computer Vision*, pages 4909–4917, 2019.
- [11] Suyog Gupta, Ankur Agrawal, Kailash Gopalakrishnan, and Pritish Narayanan. Deep learning with limited numerical precision. In *International Conference on Machine Learning*, pages 1737–1746, 2015.
- [12] Bo Han, Jiangchao Yao, Gang Niu, Mingyuan Zhou, Ivor Tsang, Ya Zhang, and Masashi Sugiyama. Masking: A new perspective of noisy supervision. In *Advances in Neural Information Processing Systems*, pages 5836–5846, 2018.
- [13] Bo Han, Quanming Yao, Xingrui Yu, Gang Niu, Miao Xu, Weihua Hu, Ivor Tsang, and Masashi Sugiyama. Co-teaching: Robust training of deep neural networks with extremely noisy labels. In *Advances in neural information processing systems*, pages 8527–8537, 2018.
- [14] Kai Han, Yunhe Wang, Yixing Xu, Chunjing Xu, Enhua Wu, and Chang Xu. Training binary neural networks through learning with noisy supervision. In *International Conference on Machine Learning*, pages 4017–4026. PMLR, 2020.
- [15] Koen Helwegen, James Widdicombe, Lukas Geiger, Zechun Liu, Kwang-Ting Cheng, and Roeland Nusselder. Latent weights do not exist: Rethinking binarized neural network optimization. In *Advances in neural information processing systems*, pages 7533–7544, 2019.
- [16] Geoffrey Hinton, Oriol Vinyals, and Jeff Dean. Distilling the knowledge in a neural network. *arXiv preprint arXiv:1503.02531*, 2015.
- [17] Furong Huang, Jordan Ash, John Langford, and Robert Schapire. Learning deep resnet blocks sequentially using boosting theory. In *International Conference on Machine Learning*, pages 2058–2067. PMLR, 2018.
- [18] Itay Hubara, Matthieu Courbariaux, Daniel Soudry, Ran El-Yaniv, and Yoshua Bengio. Binarized neural networks. *Advances in neural information processing systems*, 29:4107–4115, 2016.
- [19] Alex Krizhevsky, Geoffrey Hinton, et al. Learning multiple layers of features from tiny images. 2009.
- [20] Alex Krizhevsky, Ilya Sutskever, and Geoffrey E Hinton. Imagenet classification with deep convolutional neural networks. In *Advances in neural information processing systems*, pages 1097–1105, 2012.
- [21] Kuang-Huei Lee, Xiaodong He, Lei Zhang, and Linjun Yang. Cleannet: Transfer learning for scalable image classifier training with label noise. In *Proceedings of the IEEE Conference on Computer Vision and Pattern Recognition*, pages 5447–5456, 2018.
- [22] Mingbao Lin, Rongrong Ji, Zihan Xu, Baochang Zhang, Yan Wang, Yongjian Wu, Feiyue Huang, and Chia-Wen Lin. Rotated binary neural network. *arXiv preprint arXiv:2009.13055*, 2020.
- [23] Xiaofan Lin, Cong Zhao, and Wei Pan. Towards accurate binary convolutional neural network. In *Advances in neural information processing systems*, pages 345–353, 2017.
- [24] Chunlei Liu, Wenrui Ding, Yuan Hu, Baochang Zhang, Jianzhuang Liu, Guodong Guo, and David Doermann. Rectified binary convolutional networks with generative adversarial learning. *International Journal of Computer Vision*, pages 1–15, 2021.
- [25] Tianyi Liu, Minshuo Chen, Mo Zhou, Simon S Du, Enlu Zhou, and Tuo Zhao. Towards understanding the importance of shortcut connections in residual networks. In *Advances in neural information processing systems*, pages 7892–7902, 2019.

[26] Zechun Liu, Baoyuan Wu, Wenhan Luo, Xin Yang, Wei Liu, and Kwang-Ting Cheng. Bi-real net: Enhancing the performance of 1-bit cnns with improved representational capability and advanced training algorithm. In *Proceedings of the European conference on computer vision (ECCV)*, pages 722–737, 2018.

[27] Jian-Hao Luo, Jianxin Wu, and Weiyao Lin. Thinet: A filter level pruning method for deep neural network compression. In *Proceedings of the IEEE international conference on computer vision*, pages 5058–5066, 2017.

[28] Hyeyoung Noh, Seunghoon Hong, and Bohyung Han. Learning deconvolution network for semantic segmentation. In *Proceedings of the IEEE international conference on computer vision*, pages 1520–1528, 2015.

[29] Ini Oguntola, Subby Olubeko, and Christopher Sweeney. Slimnets: An exploration of deep model compression and acceleration. In *2018 IEEE High Performance extreme Computing Conference (HPEC)*, pages 1–6. IEEE, 2018.

[30] Wonpyo Park, Dongju Kim, Yan Lu, and Minsu Cho. Relational knowledge distillation. In *Proceedings of the IEEE Conference on Computer Vision and Pattern Recognition*, pages 3967–3976, 2019.

[31] George Philipp, Dawn Song, and Jaime G Carbonell. Gradients explode-deep networks are shallow-resnet explained. 2018.

[32] Haotong Qin, Ruihao Gong, Xianglong Liu, Mingzhu Shen, Ziran Wei, Fengwei Yu, and Jingkuan Song. Forward and backward information retention for accurate binary neural networks. In *Proceedings of the IEEE/CVF Conference on Computer Vision and Pattern Recognition*, pages 2250–2259, 2020.

[33] Stephan Rabanser, Oleksandr Shchur, and Stephan Günnemann. Introduction to tensor decompositions and their applications in machine learning. *arXiv preprint arXiv:1711.10781*, 2017.

[34] Mohammad Rastegari, Vicente Ordonez, Joseph Redmon, and Ali Farhadi. Xnor-net: Imagenet classification using binary convolutional neural networks. In *European conference on computer vision*, pages 525–542. Springer, 2016.

[35] Shaoqing Ren, Kaiming He, Ross Girshick, and Jian Sun. Faster r-cnn: Towards real-time object detection with region proposal networks. In *Advances in neural information processing systems*, pages 91–99, 2015.

[36] BRYAN RUST. Convergence of fourier series. 2013.

[37] Ying Tai, Jian Yang, and Xiaoming Liu. Image super-resolution via deep recursive residual network. In *Proceedings of the IEEE conference on computer vision and pattern recognition*, pages 3147–3155, 2017.

[38] Diwen Wan, Fumin Shen, Li Liu, Fan Zhu, Jie Qin, Ling Shao, and Heng Tao Shen. Tbn: Convolutional neural network with ternary inputs and binary weights. In *Proceedings of the European Conference on Computer Vision (ECCV)*, pages 315–332, 2018.

[39] Jiwei Yang, Xu Shen, Jun Xing, Xinmei Tian, Houqiang Li, Bing Deng, Jianqiang Huang, and Xian-sheng Hua. Quantization networks. In *Proceedings of the IEEE Conference on Computer Vision and Pattern Recognition*, pages 7308–7316, 2019.

[40] Xingrui Yu, Bo Han, Jiangchao Yao, Gang Niu, Ivor W Tsang, and Masashi Sugiyama. How does disagreement help generalization against label corruption? *arXiv preprint arXiv:1901.04215*, 2019.

[41] Zhihu Zhang and Mert Sabuncu. Generalized cross entropy loss for training deep neural networks with noisy labels. *Advances in neural information processing systems*, 31:8778–8788, 2018.

[42] Shuchang Zhou, Yuxin Wu, Zekun Ni, Xinyu Zhou, He Wen, and Yuheng Zou. Dorefa-net: Training low bitwidth convolutional neural networks with low bitwidth gradients. *arXiv preprint arXiv:1606.06160*, 2016.

[43] Zhuangwei Zhuang, Mingkui Tan, Bohan Zhuang, Jing Liu, Yong Guo, Qingyao Wu, Junzhou Huang, and Jinhui Zhu. Discrimination-aware channel pruning for deep neural networks. In *Advances in Neural Information Processing Systems*, pages 875–886, 2018.